

Accuracy of topological entanglement entropy on finite cylinders

Hong-Chen Jiang¹, Rajiv R. P. Singh², and Leon Balents¹

¹*Kavli Institute for Theoretical Physics, University of California, Santa Barbara, CA, 93106*

²*Physics Department, University of California, Davis, CA, 95616*

(Dated: January 15, 2021)

Topological phases are unique states of matter which support non-local excitations which behave as particles with fractional statistics. A universal characterization of gapped topological phases is provided by the topological entanglement entropy (TEE). We study the finite size corrections to the TEE by focusing on systems with Z_2 topological ordered state using density-matrix renormalization group (DMRG) and perturbative series expansions. We find that extrapolations of the TEE based on the Renyi entropies with Renyi index $n \geq 2$ suffer from much larger finite size corrections than do extrapolations based on the von Neumann entropy. In particular, when the circumference of the cylinder is about ten times the correlation length, the TEE obtained using von Neumann entropy has an error of order 10^{-3} , while for Renyi entropies it can even exceed 40%. We discuss the relevance of these findings to previous and future searches for topological ordered phases, including quantum spin liquids.

Topological phases are exotic states of matter that are characterized by ground state degeneracy dependent upon global topology of the system on which the phase resides, and which host exotic excitations with fractional quantum statistics. In recent years, surprising connections have emerged between topological phases and quantum information, stimulated by the prospect of using them to construct an inherently fault-tolerant quantum computer[1, 2]. Two dimensional phases with topological order are well known in connection with the fractional quantum Hall effect[3], but are also expected to exist in frustrated quantum magnets[4, 5].

While topological phases are not characterized by any *local* order parameter, theory shows that they can be identified by non-local quantum entanglement, specifically the topological entanglement entropy (TEE) of the ground states[6, 7]. The entanglement entropy of a subregion A of the system with a smooth boundary of length L is defined from the reduced density matrix ρ_A , according to

$$S_1(A) = -\text{Tr}[\rho_A \ln(\rho_A)],$$

and takes the form

$$S_1(A) = \alpha_1 L - \gamma,$$

where γ is the TEE. Severe finite-size corrections of the formulations in Ref.[6, 7] due to lattice-scale effects greatly hinder their practical application[8]. Instead, two of us have recently proposed a practical and extremely simple scheme, the “cylinder construction”, to accurately calculate TEE[9]. The cylinder construction simply consists of using the DMRG[10] to calculate the usual von Neumann entanglement entropy for the division of a cylinder into two equal halves by a flat cut, and extracting the TEE from its asymptotic large-circumference limit. Thereby, we can practically identify topological phases in arbitrary realistic models, including physical spin models[9, 11].

The work above utilized the von Neumann entanglement entropy, and achieved an accurate extrapolation of the TEE term. In the literature, many works study instead the generalized Renyi entropies, defined as

$$S_n(A) = \frac{1}{1-n} \ln \text{Tr} \rho_A^n,$$

while the von Neumann entropy S_1 is defined as the limit $n \rightarrow 1$. For simplicity, we will call S_n as Renyi entanglement entropy when $n \geq 2$, while von Neumann entanglement entropy when $n = 1$. Theoretically, the universal TEE is expected to obtain also for the Renyi entropy, with γ independent of the Renyi index. However, extrapolations in the literature based on the Renyi entropy appear to be substantially less accurate than those based on the von Neumann entropy, even for larger boundary lengths L [12]. In particular, the extrapolated TEE in Ref.[12] from the second-order Renyi entropy S_2 deviates from the expected value with an error an order of magnitude larger than that from von Neumann entanglement entropy S_1 [9]. This suggests that extrapolations of Renyi entropies have significantly larger finite-size effects than von Neumann entropy.

In this letter, we study the finite-size effects in the TEE systematically for two canonical models of phases with Z_2 topological order, and confirm the above suggestion. We attempt to cast our results in terms of the expected form,

$$S_n(L) = \alpha_n L - \gamma_n, \quad (1)$$

as a function of Renyi index n . First, we study the Toric-Code model whose TEE is known, using DMRG and perturbative series expansions[13]. We then turn to the more realistic $S = 1/2$ antiferromagnetic Heisenberg model on the Kagome lattice. For both cases, we find that the Renyi entropies do have substantially larger finite-size corrections than the von Neumann entropy. We provide some understanding of this tendency from the fact, which we show from the series expansion, that the line term α_n

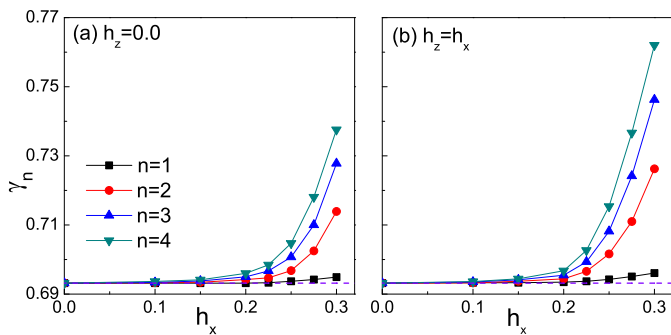


FIG. 1: (Color online) The extrapolated TEE γ_n using von Neumann entropy (i.e., $n = 1$) and Renyi entropy (i.e., $n \geq 2$) for the Toric-Code model, as a function of the applied magnetic field h_x , for (a) $h_z = 0$ and (b) symmetric case $h_z = h_x$. The dashed lines represent the expected universal value, $\ln 2$, for the TEE in the thermodynamic limit.

varies more rapidly with parameters with increasing n . This makes the extraction of the sub-dominant γ_n term less reliable.

Toric-Code Model We begin with the well known Toric-Code model (TCM)[1], (See Supplementary Information for notational details). Without applied fields, i.e., $h_x = h_z = 0$, the pure TCM is exactly soluble[1] with a Z_2 topological ordered ground state. After turning on the magnetic fields, the model is no longer exactly soluble. Previous studies [14–16] show that the Z_2 topological phase remains stable and robust until the magnetic fields are large enough that the system undergoes a phase transition from the topological phase to a trivial one. Numerically, Jiang, Wang and Balents have systematically calculated the von Neumann entanglement entropy S_1 using cylinder construction[9], and extrapolated an accurate TEE $\gamma_1 = \ln(2)$ in the Z_2 topological phase, even very close to the phase transition point. In this paper, we further calculate the Renyi entropy to study the finite-size effects on the TEE γ_n as a function of Renyi index n . To make sure that S_n only scales with the cylinder circumference $L_y = L$, we will work in the long cylinder limit, i.e., cylinder length $L_x \rightarrow \infty$. Therefore, we can directly extrapolate the TEE γ_n using Eq.(1).

To see the finite-size corrections, we first consider an applied magnetic field only along x -direction, i.e., $h_z = 0$. The extrapolated TEE γ_n are shown in Fig.1 (a) as a function of magnetic field h_x for fields within the topological phase. As shown in the Supplementary Material, for the fields in Fig. 1, the spin correlation length remains of order one lattice spacing or smaller. We see that the linear fit using data for $L_y = 6 \sim 12$ and Eq.(1) gives quite accurate results for γ_1 for $h_x < h_x^c \approx 0.328$ [14]. Even for $h_x = 0.3$, very close to the quantum phase transition, we obtain $\gamma_1 = 0.6945(20)$, which is accurate to the expected value (i.e., the dashed line) to a fraction of percent $\sim 0.2\%$. By contrast, the estimated TEE γ_n

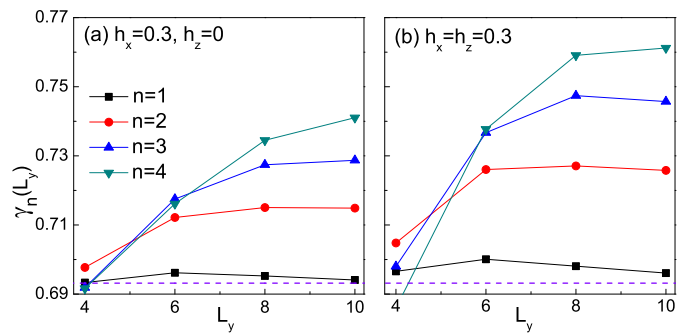


FIG. 2: (Color online) Moving two point data fits for the extrapolated TEE γ_n for the Toric-Code model for (a) $h_x = 0.3$ with $h_z = 0$, and (b) $h_x = h_z = 0.3$, as a function of the cylinder circumference L_y and entropy index n . Here, $\gamma_n(L_y)$ are fitted using two data points, i.e., $S_n(L_y)$ and $S_n(L_y + 2)$ using Eq.(1). The dashed lines represent the expected asymptotic value $\gamma = \ln 2$.

obtained from the Renyi entropy for $n \geq 2$ shows dramatically larger deviations from the universal value. These deviations grow when approaching the phase transition point, where the errors become an order of magnitude larger than those for γ_1 . For example, $\gamma_2 = 0.714(5)$ at $h_x = 0.3$, with an error around $\sim 3\%$. The deviations also increase with Renyi index n , e.g., $\sim 7\%$ for $n = 4$, as shown in Fig.1 (a) and inset of Fig.4. Similar results hold for the symmetric case $h_x = h_z$, with even larger finite-size corrections, as shown in Fig.1(b) and inset of Fig.4. Systematically, the finite-size corrections to the TEE γ_n defined by Eq.(1) are much larger for the Renyi entropy than for the von Neumann entropy.

Our expectation is that *in the thermodynamic limit* $L_y \rightarrow \infty$, all γ_n should converge properly to the universal value. We look for signs of this tendency, by using a moving two data-point fit. We can define $\gamma_n(L_y)$ using two data points with different cylinder circumferences L_y and $L_y + 2$. Examples of such $\gamma_n(L_y)$ are shown in Fig.2 for $h_x = 0.3$ and $h_z = 0$ in (a), and for $h_x = h_z = 0.3$ in (b), as a function of L_y . For both cases, $\gamma_1(L_y)$ quickly converges to the expected value, which is in sharp contrast to $\gamma_n(L_y)$ using Renyi entropies with $n \geq 2$. For the latter cases, the TEE is systematically over-estimated. The curves in Fig. 2 do at least show downward curvature, consistent with eventual convergence to the universal value for larger L_y , but it is clear the much larger systems would be required to test this in detail.

To understand the origin of the n -dependence in the extrapolations, we turn to a perturbative series expansion calculation of the line term α_n . Since the TEE is obtained after subtraction of the much larger line term, an accurate extrapolation of γ_n also requires an accurate calculation of α_n . While there have been perturbative studies of the Kitaev model in a field[17] and some entanglement properties have also been studied[18, 19], we are

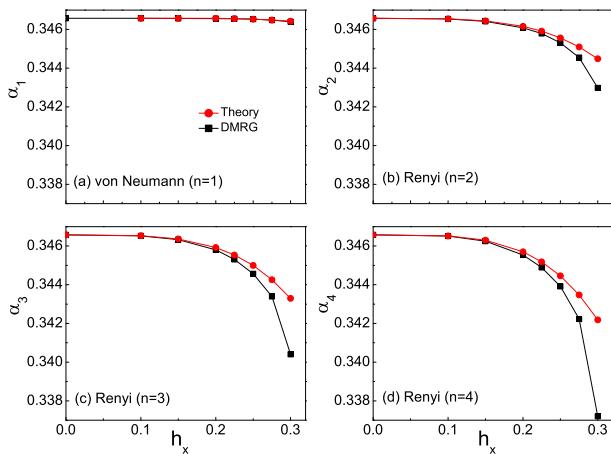


FIG. 3: (Color online) Line entropy α_n obtained from DMRG (block square) and perturbative calculation (red circle) for both von Neumann entropy (i.e., $n = 1$) and Renyi entropy (i.e., $n \geq 2$) for the Toric-Code model, as a function of the magnetic field h_x , here $h_z = 0$.

not aware of any exact perturbative evaluation of its line entropy relevant to our geometry. In order to carry out this calculation, we turn to Linked Cluster Methods.[13]

We consider one of the ground state sectors of the TCM and map the problem on to the Transverse-Field Ising Model (TFIM) if only h_x is non-zero[14] and on to a Z_2 Lattice-gauge model if both h_x and h_z are non-zero.[16] In either case, one has a unique non-degenerate ground state. Here, we will consider only the former mapping and the case with only h_x non-zero. Up to 4-th order, the dependence on h_x and h_z are additive and hence knowing the dependence on h_x and the symmetry under the interchange of h_x and h_z one can easily write down the full dependence on h_x and h_z .

Given the exact mapping between the models, if we were to calculate some property like the ground state energy in a series expansion in the field, the expansions would be identical to the TFIM. However, there is a crucial difference for the entanglement entropies.[20] The TFIM variables sit at the center of the plaquettes whereas the TCM variables and the perturbing fields live on the bonds. Furthermore, each state in the TCM is a linear superposition of many basis states (say in the σ_z basis). This affects how the states are represented on either side of the partition and hence the reduced density matrix as we discuss below.

In the linked cluster method, we can define a cluster by a set of bonds, where the perturbative fields are present.[21, 22] The entanglement entropies can be expressed as

$$S_n = \sum_c W_n(c), \quad (2)$$

where the sum is over all possible clusters c and the

weight of a cluster $W_n(c)$ is defined recursively by the relations

$$W_n(c) = S_n(c) - \sum_s W_n(s), \quad (3)$$

where $S_n(c)$ is the entanglement entropy for the cluster c and the sum over s is over all subclusters of c .

One can show that, for the line entropy, the only clusters that will give non-zero contributions in powers of h are those that are (i) linked and (ii) that contain at least one bond in subsystem A and one in subsystem B.[21, 22] Here, one should note that two bonds are linked if they meet at a site or if they are on the opposite sides of an elementary plaquette (because they can both change the flux through a common plaquette). This implies that all such clusters must be situated close to the interface between A and B. Since such linked clusters can be translated along the line, it follows that, for a large system, this entropy is proportional to the length of the line. In fourth order, we can group the perturbations into just two distinct clusters, whose calculational details can be found in the Supplementary materials.

For line term of the Renyi entropy for $n > 1$, to order h^4 , we obtain

$$\alpha_n = \frac{1}{2}(\ln 2 - \frac{9n}{32}h^4 + \frac{3n}{n-1} \frac{h^4}{128}) \quad (4)$$

while, the von-Neumann entropy ($n \rightarrow 1$) becomes

$$\alpha_1 = \frac{1}{2}(\ln 2 - (\frac{33}{128} - \frac{5}{32} \ln 2)h^4 - \frac{3}{32}h^4 \ln h). \quad (5)$$

Note that the innocuous $h^n \ln h$ singularity is inevitable for the von-Neumann entropy in any model, where there are Schmidt states, whose weight is zero in the unperturbed model but becomes non-zero as a power of the perturbation parameter.

In Fig.3 we show the line entropies α_n obtained in DMRG compared with the series expansion results (See also Fig.S3 in Supplementary materials). The agreement is excellent. The important thing to note is the n dependence of the line entropy. The linear n dependence in Eq.(4) means that with increasing n , the line entropy changes more rapidly with the applied fields. Since, the topological entanglement entropy is obtained after subtraction of the much larger line entropy, it follows that with increasing n the entanglement entropy would have a much larger finite size correction, as the correlation length increases.

Kagome Heisenberg Model We now turn to the spin-1/2 Heisenberg model on the Kagome lattice, for which compelling[23, 24] and direct evidence[9, 12] for a Z_2 topological quantum spin liquid has been obtained by extensive DMRG studies. In particular, highly accurate TEE $\gamma_1 = \ln(2)$ has been obtained using cylinder construction[9], for the model with both first- and

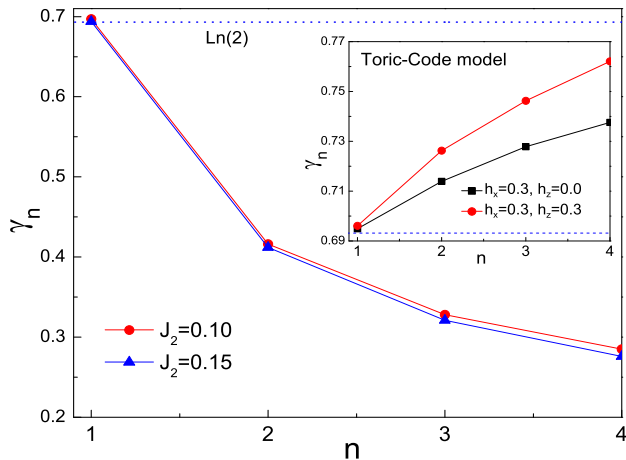


FIG. 4: (Color online) The extrapolated TEE γ_n for the Kagome J_1 - J_2 Heisenberg model as a function of entropy index n at both $J_2 = 0.10$ and $J_2 = 0.15$. Inset: γ_n for TCM as a function of entropy index n , for the case $h_x = 0.3, h_z = 0$ (black square), and the symmetric case $h_x = h_z = 0.3$ (red circle). The dashed lines correspond to $\ln(2)$.

second-neighbor interactions – see the Supplementary Information for details of the definition. Specifically, the extrapolated TEE $\gamma_1 = 0.698(8)$ at $J_2 = 0.10$ and $\gamma_1 = 0.694(6)$ at $J_2 = 0.15$, both within one percent of $\ln(2) = 0.693$.

As in the TCM, we find that the Renyi entropies give much less accurate estimates of γ_n . The extrapolated TEE γ_n for $n \geq 2$ clearly deviates from the expected value, even when the cylinder circumference is much larger than the correlation length, i.e., $L_y \approx 10\xi$ (the correlation lengths are known from the earlier study in Ref.[9]). For example, as shown in Fig.S5, a linear fit using Eq.(1) gives $\gamma_2 \approx 0.42(1)$ at both $J_2 = 0.10$ and $J_2 = 0.15$: a huge error of $\sim 40\%$. Moreover, with increasing Renyi index n , the deviation becomes even larger, reaching, for example $\sim 60\%$ for $n = 4$, as shown in Fig.4. These results show that large finite-size corrections to the Renyi entropies obtain not only in the “artificial” TCM, but also in realistic quantum spin Hamiltonians.

Summary and Conclusion In this paper, we studied the finite-size scaling of the TEE for systems with Z_2 topological order, using DMRG simulations and perturbative series expansions. We find that generally the finite-size errors in the TEE based on the Renyi entropy estimators (i.e., $n \geq 2$) are much larger than those obtained from the von Neumann entropy (i.e., $n = 1$). In particular, when the cylinder circumference is around ten times the correlation length, $L_y \approx 10\xi$, the extrapolated TEE using von Neumann entropy is quite accurate with an error of order 10^{-3} . On the contrary, the error can be orders of magnitude larger for Renyi entropy. For in-

stance, for spin-1/2 Kagome Heisenberg model, the error is only around a fraction of percent for von Neumann entropy, while it is 40% or even larger for Renyi entropy. Perturbative study of the TCM shows that the larger finite size corrections for the TEE originates in part from the enhanced variation with parameters of the line entropy α_n with increasing n . This indicates moreover that estimates of the TEE become less accurate with increasing n . We note that errors of the magnitude found here for $n \geq 2$ in the Kagome Heisenberg model are large enough to perhaps preclude a definitive identification of the topological phase, even if we *assume* that a universal value obtains in the thermodynamic limit. Our results clearly indicate that great care must be taken into account for finite size corrections in numerical calculations of the TEE, particularly those based on Renyi entropies with $n \geq 2$. This gives techniques, such as DMRG, which have direct access to the full density matrix and hence von Neumann entropy, a distinct advantage. Although in this paper we have focused on systems with Z_2 topological order, similar conclusions may be expected more generally.

Acknowledgement HCJ thanks Andreas Ludwig for helpful discussion and Zhengnan Wang for early collaboration. We acknowledge computing support from the Center for Scientific Computing at the CNSI and MRL: an NSF MRSEC (DMR-1121053) and NSF CNS-0960316. This research was supported in part by DMR-1004231 (RRPS) and DMR-1206809 (LB) and the KITP NSF grant PHY-1125915 (HCJ, LB, RRPS).

-
- [1] A. Y. Kitaev, Ann. Phys. (N.Y.) **303**, 2 (2003).
 - [2] C. Nayak, S. H. Simon, A. Stern, M. Freedman, and S. Das Sarma, Rev. Mod. Phys. **80**, 1083 (2008).
 - [3] R. B. Laughlin, Phys. Rev. Lett. **50**, 1395 (1983).
 - [4] P. W. Anderson, Materials Research Bulletin **8**, 153 (1973).
 - [5] L. Balents, Nature **464**, 199 (2010).
 - [6] A. Kitaev and J. Preskill, Phys. Rev. Lett. **96**, 110404 (2006).
 - [7] M. Levin and X.-G. Wen, Phys. Rev. Lett. **96**, 110405 (2006).
 - [8] S. Furukawa and G. Misguich, Phys. Rev. B **75**, 214407 (2007).
 - [9] H. C. Jiang, Z. Wang, and L. Balents, Nature Physics **8**, 902 (2012).
 - [10] S. R. White, Phys. Rev. Lett. **69**, 2863 (1992).
 - [11] H. C. Jiang, H. Yao, and L. Balents, Phys. Rev. B **86**, 024424 (2012).
 - [12] S. Depenbrock, I. P. McCulloch, and U. Schollwöck, Phys. Rev. Lett. **109**, 067201 (2012).
 - [13] J. Oitmaa, C. Hamer, and W. Zheng, Cambridge University Press (2006).
 - [14] S. Trebst, P. Werner, M. Troyer, K. Shtengel, and C. Nayak, Phys. Rev. Lett. **98**, 070602 (2007).
 - [15] J. Vidal, S. Dusuel, and K. P. Schmidt, Phys. Rev. B **79**,

- 033109 (2009).
- [16] I. S. Tupitsyn, A. Kitaev, N. V. Prokof'ev, and P. C. E. Stamp, Phys. Rev. B **82**, 085114 (2010).
- [17] J. Vidal, S. Dusuel, and K. P. Schmidt, Phys. Rev. B **79**, 033109 (2009).
- [18] S. Papanikolaou, K. S. Raman, and E. Fradkin, Phys. Rev. B **76**, 224421 (2007).
- [19] G. B. Halász and A. Hama, Phys. Rev. A **86**, 062330 (2012).
- [20] A. B. Kallin, K. Hyatt, R. R. P. Singh, and R. G. Melko, arXiv:1212.5269 (2012).
- [21] R. R. P. Singh, R. G. Melko, and J. Oitmaa, Phys. Rev. B **86**, 075106 (2012).
- [22] M. P. Gelfand, R. R. P. Singh, and D. A. Huse, J. Stat. Phys. **59**, 1093 (1990).
- [23] H. C. Jiang, Z. Y. Weng, and D. N. Sheng, Phys. Rev. Lett. **101**, 117203 (2008).
- [24] S. Yan, D. Huse, and S. White, Science **332**, 1173 (2011).

Supplementary Information

I. Toric-Code Model in Magnetic Field

The Toric-Code model[1] with an applied magnetic field is given by

$$H = -J_s \sum_s A_s - J_p \sum_p B_p - h_x \sum_i \sigma_i^x - h_z \sum_i \sigma_i^z \quad (\text{S1})$$

where σ_i^x and σ_i^z are Pauli matrices, $A_s = \prod_{i \in s} \sigma_i^x$ and $B_p = \prod_{i \in p} \sigma_i^z$. Subscripts s and p refer respectively to vertices and plaquettes on the square lattice, whereas i runs over all bonds where spin degrees of freedom are located. Without magnetic field, i.e., $h_x = h_z = 0$, the pure TCM can be solved exactly[1]. It exhibits a 4-fold ground state degeneracy on the torus, and has Z_2 topological order with total quantum dimension $D = 2$. All elementary excitations are gapped and characterized by eigenvalues $A_s = -1$ (a Z_2 charge on site s) and $B_p = -1$ (a Z_2 vortex on plaquette p). After turning on the magnetic fields, the model cannot be solved exactly anymore. However, previous studies[14–16] show that the Z_2 topological phase remains quite stable and robust until the magnetic fields are large enough to induce a phase transition from the topological phase to the trivial one. Specifically, such a phase transition takes place at the critical magnetic field $h_x^c \approx 0.32$ when $h_z = 0$, while $h_x^c \approx 0.34$ along the symmetric line with $h_z = h_x$.

For the DMRG simulation, we consider an equivalent square lattice, where the spin operators σ^x and σ^z sit on the sites instead of the bonds. Therefore, the star operator A_s and the plaquette operator B_p of the original lattice now sit on alternating plaquettes in the equivalent square lattice, as shown in Figure S1, labeled as S and P , respectively. Note that on this equivalent square lattice, there are an even number of dangling spins within each plaquette at the open edges. For the pure Toric-Code model with cylinder boundary condition, the first

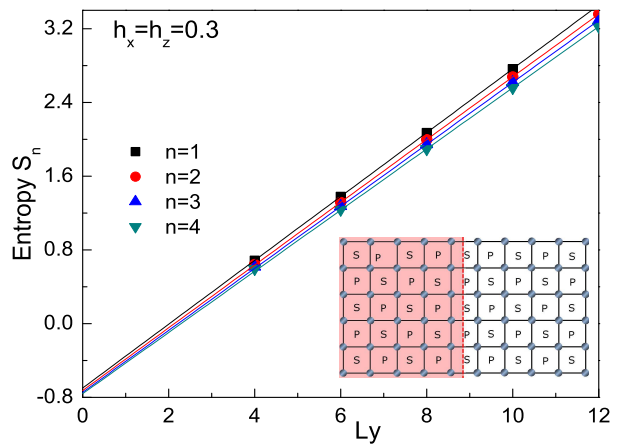


FIG. S1: The entanglement entropy for the Toric-Code model in magnetic fields $h_x = h_z = 0.3$ in Eq.(S1), with $L_y = 4 \sim 12$ at $L_x = \infty$. Here n is the entropy index. Inset: Square lattice with $L_x = 10$ and $L_y = 6$. Here S represents the star operator A_s , while P represents the plaquette operator B_p .

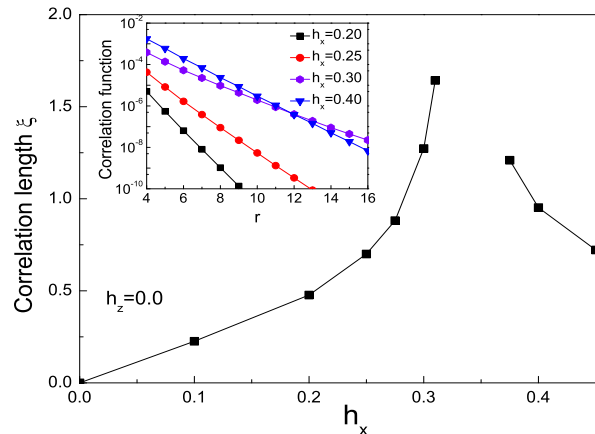


FIG. S2: The spin-spin correlation length for the Toric-Code model as a function of the applied magnetic field h_x in Eq.(S1), with $h_z = 0.0$. Inset: Examples of spin-spin correlation function $\langle \tilde{\sigma}_0^x \tilde{\sigma}_r^x \rangle = \langle \sigma_0^x \sigma_r^x \rangle - \langle \sigma_0^x \rangle \langle \sigma_r^x \rangle$ along the cylinder, at different magnetic field h_x .

$2^{L_y/2-1}$ eigenvalues of the reduced density matrix ρ_A are degenerate and equal to $1/2^{L_y/2-1}$, while all the other eigenvalues are zero. Therefore, the entanglement entropy, defined as $S_n = \frac{1}{n-1} \ln \text{Tr} \rho_A^n$, does not depend on the entropy index n , and is equal to $S_n = \frac{\ln(2)}{2} L_y - \ln(2)$, with coefficient $\alpha_n = \ln(2)/2$ and TEE $\gamma_n = \ln(2)$.

After turning on the magnetic field, the degeneracy of entanglement spectrum is lifted, and the correlation length ξ becomes finite, as shown in Fig.S2 (note that other types of the correlation length may be defined, but are expected to differ just by a factor of order 1 from the above one). Therefore, the entanglement entropy S_n will depend on the entropy index n , and it follows that

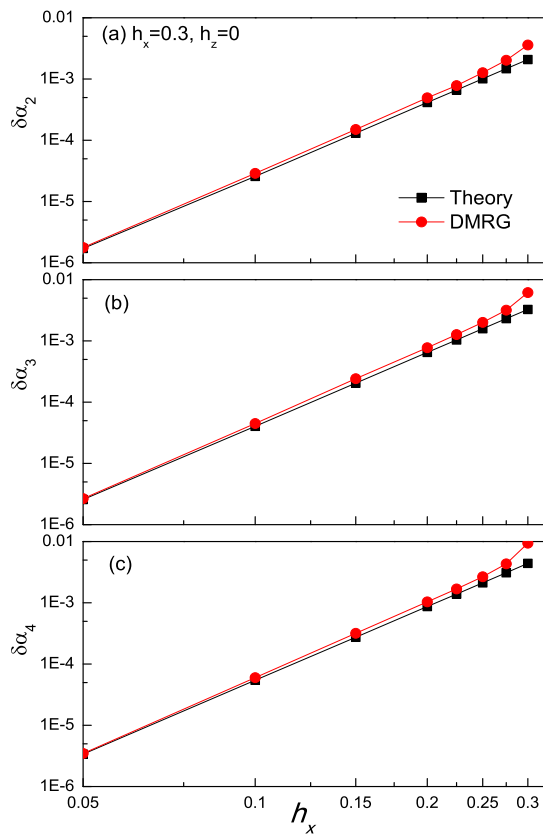


FIG. S3: Deviation of the coefficient $\delta\alpha_n \equiv \alpha_n(h_x = 0) - \alpha_n(h_x)$ obtained from DMRG using Eq.(1) (red circle) and theoretical formula in Eq.(4) up to 4th order series expansion for Renyi entropy (black square) with (a) $n = 2$, (b) $n = 3$ and (c) $n = 4$ for the Toric-Code model, as a function of the applied magnetic field h_x . Here $h_z = 0$.

so too will the coefficient α_n and the extrapolated TEE γ_n . Indeed, our results show that when approaching the phase transition point (e.g., $h_x^c = 0.34$ along the symmetric line with $h_x = h_z$), the dependence of the TEE γ_n on n becomes clearer and clearer, as shown in Fig.1(b) in the main text, and Fig.S1 here. For example, the correlation length $\xi \approx 1$ lattice spacing at $h_x^c = 0.30$, and the resulting TEE $\gamma_1 = 0.696(4)$ obtained from the von Neumann entanglement entropy is still quite accurate with an error around a few fraction of 10^{-3} , i.e., $\sim 0.4\%$. On the contrary, the fitted TEE γ_n using Renyi entropy (i.e., $n \geq 2$) deviates from the expected value clearly, with an error more than order of magnitude larger than for γ_1 . For instance, $\gamma_2 = 0.726(6)$, with an error around 5%, around one order of magnitude larger than that for γ_1 . Such a deviation is even larger with the increase of n , e.g., $\gamma_4 = 0.762(8)$, with an error around 10%, more than one order of magnitude larger than that for γ_1 .

Deviations are also found in the line entropies α_n . Fig.S3 shows the comparison for α_n obtained numerically using Eq.(1) and theoretically using Eq.(4) up to 4th order

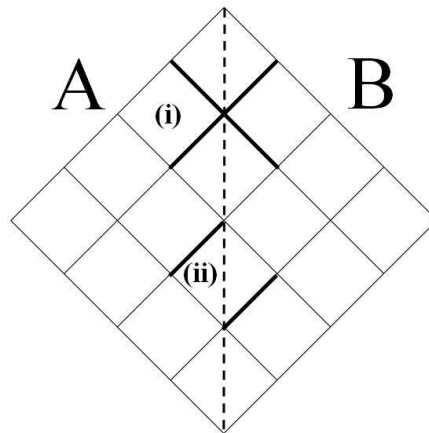


FIG. S4: Graphs needed for the perturbative calculation of the line entropy to 4th order. The dashed line separates subsystems A and B. The solid lines denote the perturbing fields in the cluster.

der series expansion. The series expansion results match the DMRG values remarkably accurately, though as expected, the difference between the two increases markedly on approaching the phase transition point, especially for larger n .

II. Perturbative calculations

The perturbative calculations to order h^4 for the Toric Code Model require just two clusters shown in Fig.S4: (i) A cluster consisting of all four bonds incident on a boundary site between A and B and (ii) A cluster with two bonds across a plaquette facing each other across the boundary between A and B. The first has a count of one per boundary site. The second has a count of 2 per boundary site. Once grouped this way, no subgraph subtraction is needed in 4th order.

We now discuss the calculation of $S_n(c)$, the Renyi entropy when only the fields on the bonds of a cluster c are present.[22] First the ground state wavefunction is calculated perturbatively in the TFIM variables, with all the perturbing fields present in the cluster. Then, for every basis state in the TFIM model, a representative σ_z basis state is obtained in the TCM variable. When all the 4 perturbative fields are present at a site, the states in the TCM must be enlarged by the operation of the projection operator $1 + A_s$ at the site. This will give us the ground state for the cluster in the TCM variables. Once, the ground state for the cluster is known in the TCM variables, it is straightforward to calculate the reduced density matrix for subsystem A and hence the entanglement entropies, $S_n(c)$.

First we consider graph (ii) from the figure. This graph has just two bonds, one in A and one in B. In the lan-

guage of TFIM, there are three plaquettes on which Visions can be created or destroyed. However, since Visions are created or destroyed in pairs, there are only 4 relevant states in the Hilbert space. These can be denoted by the number of Visions present in the plaquette as $|1\rangle = |0,0,0\rangle$, $|2\rangle = |1,1,0\rangle$, $|3\rangle = |0,1,1\rangle$ and $|4\rangle = |1,0,1\rangle$. These four states can be related to the TCM in terms of σ_z on the two bonds of the cluster. The four states become $|1\rangle = |1,1\rangle$, $|2\rangle = |-1,1\rangle$, $|3\rangle = |1,-1\rangle$ and $|4\rangle = |-1,-1\rangle$. In this 4-dimensional Hilbert space, the Hamiltonian matrix is

$$H = \begin{pmatrix} 0 & -h & -h & 0 \\ -h & 4 & 0 & -h \\ -h & 0 & 4 & -h \\ 0 & -h & -h & 4 \end{pmatrix}.$$

The ground state wavefunction correct to order required for h^4 evaluation of Renyi entropies is

$$\psi_g = \begin{pmatrix} 1 - \frac{h^2}{16} - \frac{h^4}{512} \\ \frac{h}{4} - \frac{h^3}{64} \\ \frac{h}{4} - \frac{h^3}{64} \\ \frac{h^2}{8} + O(h^4) \end{pmatrix}.$$

Let A_i label the basis states for subsystem A and B_k label basis states for subsystem B . Then reduced density matrix for subsystem A has matrix elements

$$(\rho_A)_{A_i, A_j} = \sum_{B_k} \psi_{A_i, B_k} \psi_{A_j, B_k} \quad (S2)$$

In the TCM representation, there are just two states on the A side, and the reduced density matrix becomes

$$\rho_A = \begin{pmatrix} 1 - \frac{h^2}{16} - \frac{h^4}{128} & \frac{h}{4} \\ \frac{h}{4} & \frac{h^2}{16} + \frac{h^4}{128} \end{pmatrix}.$$

From this it follows that the two eigenvalues of the reduced density matrix are $1 - \frac{h^4}{256}$ and $\frac{h^4}{256}$. It leads to Renyi entanglement entropy of

$$S_n^{(ii)} = \frac{1}{1-n} \left[-\frac{nh^4}{256} + \left(\frac{h^4}{256} \right)^n \right].$$

Now, we turn to graph (i) in figure, which has 4 bonds all sharing a boundary site between A and B . There are 4 plaquettes on which Visions can be created or destroyed. But, because they are created or destroyed in pairs, there number is conserved modulo 2. Thus, there are 8 relevant basis states. We can order the plaquettes in a clockwise manner. Then the 8 states are: $|1\rangle = |0,0,0,0\rangle$, $|2\rangle = |1,1,0,0\rangle$, $|3\rangle = |0,1,1,0\rangle$, $|4\rangle = |0,0,1,1\rangle$, $|5\rangle = |1,0,0,1\rangle$, $|6\rangle = |1,1,1,1\rangle$, $|7\rangle = |1,0,1,0\rangle$ and $|8\rangle = |0,1,0,1\rangle$. The 8-dimensional Hamiltonian

matrix is given by

$$H = \begin{pmatrix} 0 & -h & -h & -h & -h & 0 & 0 & 0 \\ -h & 4 & 0 & 0 & 0 & -h & -h & -h \\ -h & 0 & 4 & 0 & 0 & -h & -h & -h \\ -h & 0 & 0 & 4 & 0 & -h & -h & -h \\ -h & 0 & 0 & 0 & 4 & -h & -h & -h \\ 0 & -h & -h & -h & -h & 8 & 0 & 0 \\ 0 & -h & -h & -h & -h & 0 & 4 & 0 \\ 0 & -h & -h & -h & -h & 0 & 0 & 4 \end{pmatrix}.$$

It leads to ground state wave function needed for 4th order calculation of Renyi entropies of:

$$\psi_g = \begin{pmatrix} 1 - \frac{h^2}{8} - \frac{9h^4}{64} \\ \frac{h}{4} + \frac{h^3}{16} \\ \frac{h}{4} + \frac{h^3}{16} \\ \frac{h}{4} + \frac{h^3}{16} \\ \frac{h}{4} + \frac{h^3}{16} \\ \frac{h^2}{8} + O(h^4) \\ \frac{h^2}{4} + O(h^4) \\ \frac{h^2}{4} + O(h^4) \end{pmatrix}.$$

Transforming to the TCM variables σ_z , there are 4 states on the A side, and remembering that each TFIM state is a superposition of two TCM basis states after applying the projection operator $(1+A_s)$, the 4×4 reduced density matrix becomes:

$$2\rho_A = \begin{pmatrix} 1 - \frac{h^2}{8} - \frac{9h^4}{64} & \frac{h}{4} + \frac{3h^3}{16} & \frac{h}{4} + \frac{3h^3}{16} & \frac{5h^2}{8} \\ \frac{h}{4} + \frac{3h^3}{16} & \frac{h^2}{8} + \frac{9h^4}{64} & \frac{h^2}{4} & \frac{h}{4} + \frac{3h^3}{16} \\ \frac{h}{4} + \frac{3h^3}{16} & \frac{h^2}{4} & \frac{h^2}{8} + \frac{9h^4}{64} & \frac{h}{4} + \frac{3h^3}{16} \\ \frac{5h^2}{8} & \frac{h}{4} + \frac{3h^3}{16} & \frac{h}{4} + \frac{3h^3}{16} & 1 - \frac{h^2}{8} - \frac{9h^4}{64} \end{pmatrix}.$$

From this it follows that the eigenvalues of $2\rho_A$ are $1 - \frac{3h^2}{4} - \frac{9h^4}{64}$, $1 + \frac{3h^2}{4} + \frac{7h^4}{64}$, $\frac{h^4}{64}$ and $\frac{h^4}{64}$. These lead to Renyi entanglement entropies:

$$S_n^{(i)} = \ln 2 - \frac{9n}{32} h^4 + \frac{1}{1-n} [(h^4/64)^n - n(h^4/64)].$$

Note that this graph also gives the full line entropy of the unperturbed TCM, which is $\ln 2$ for every site that is shared between subsystems A and B . For the unperturbed model, it is easily shown that any larger graph will give zero upon subgraph subtraction as no additional degeneracy arises on the line.

III. Kagome Heisenberg Model

The spin-1/2 Heisenberg model on the Kagome lattice, with both first- and second-neighbor interactions, is given by

$$H = J_1 \sum_{\langle ij \rangle} \mathbf{S}_i \cdot \mathbf{S}_j + J_2 \sum_{\langle\langle ij \rangle\rangle} \mathbf{S}_i \cdot \mathbf{S}_j. \quad (S3)$$

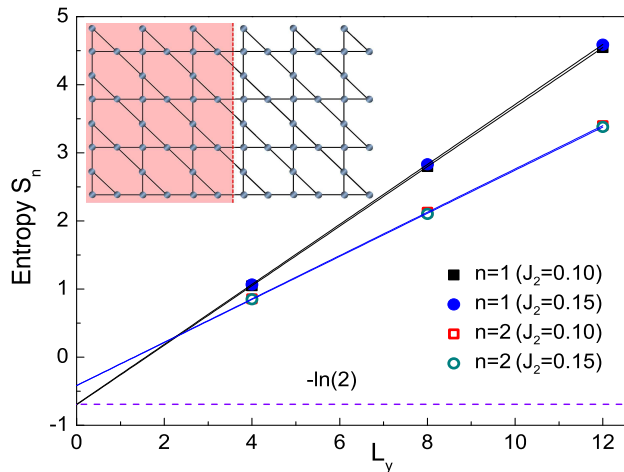


FIG. S5: The entanglement entropy $S_n(L_y)$ for the Kagome J_1 - J_2 model in Eq.(S3), with $L_y = 4 \sim 12$ at $L_x = \infty$. By fitting $S_n(L_y) = \alpha_n L_y - \gamma_n$, we get $\gamma_1 = 0.698(8)$ at $J_2 = 0.10$, and $\gamma_1 = 0.694(6)$ at $J_2 = 0.15$, while $\gamma_2 \approx 0.42(1)$ at both $J_2 = 0.10$ and 0.15 . Here n is the entropy index. Inset: Kagome lattice with $L_x = 12$ and $L_y = 8$.

Here \mathbf{S}_i is the spin operator on site i , and $\langle ij \rangle$ ($\langle\langle ij \rangle\rangle$) denotes the nearest neighbors (next nearest neighbors). In the numerical simulation, we set $J_1 = 1$ as the unit of energy. We take the kagomé lattice with periodic boundary conditions along a bond direction to define a cylinder, drawn vertically in the inset of Fig. S5, and the unit of length equal to the nearest-neighbor distance. The results for the entanglement entropy for $J_2 = 0.10$ and 0.15 are shown in Fig. S5, for which both spin-spin and dimer-dimer correlation lengths are approximately one lattice spacing[9]. We see that a linear fit using data for $L_y = 4 \sim 12$ using Eq.(1) gives $\gamma = 0.698(8)$ at $J_2 = 0.10$ and $\gamma = 0.694(6)$ at $J_2 = 0.15$, both within one percent of $\ln 2 = 0.693$. In contrast, the extrapolated TEE γ_n based on the Renyi entropy (i.e., $n \geq 2$) clearly deviates from the expected value, although the cylinder's circumference is much larger than the correlation length, i.e., $L_y \approx 10\xi$. For example, as shown in Fig.S5, a linear fit using Eq.(1) gives us $\gamma_2 \approx 0.42(1)$ at both $J_2 = 0.10$ and $J_2 = 0.15$, which differs from the expected value by an $\approx 40\%$ error.